Int. J. Electrochem. Sci., 15 **(2020)** 3157 – 3163, doi: 10.20964/2020.04.20

International Journal of
ELECTROCHEMICAL
SCIENCE
www.electrochemsci.org

Short Communication

Electrochemical Properties of Lutetium and Zirconium co-doped $SrCeO_3$ Composite Electrolyte for Intermediate Temperature for Solid Oxide Fuel Cell

Wenli Hu[1], *Wei Chen*[1], *Hongtao Wang*[1,2,*]

[1] Fuyang Preschool Education College, Fuyang 236015, China
[2] School of Chemical and Material Engineering, Fuyang Normal University, Fuyang 236037, China
[*]E-mail: hongtaoking3@163.com

Received: 16 December 2019 / *Accepted:* 6 February 2020 / *Published:* 10 March 2020

In this study, $SrCe_{0.6}Zr_{0.3}Lu_{0.1}O_{3-\alpha}$ was synthesized by a citric-nitrate auto-combustion (CNA) method. Subsequently, it was compounded with molten chlorides and carbonates to prepare $SrCe_{0.6}Zr_{0.3}Lu_{0.1}O_{3-\alpha}$-$(K/Li)_2CO_3$-(Na/K)Cl. The structure, morphology and medium temperature electrical properties of SCZLu-$(K/Li)_2CO_3$-(Na/K)Cl were investigated. X-ray diffraction indicated that the main microstructure was $SrCeO_3$ phase and $(K/Li)_2CO_3$ mainly existed in amorphous form in the composite. The maximum conductivity of SCZLu-$(K/Li)_2CO_3$-(Na/K)Cl reached 2.5×10^{-2} $S\cdot cm^{-1}$ at 700 °C.

Keywords: Composite; Electrolyte; Fuel cell; Conductivity

1. INTRODUCTION

Proton conductors have wide application prospects in the energy, environmental protection and aerospace fields etc. [1–5]. Proton conducting solid electrolytes include polymer organic film, inorganic heteropoly acid and ABO_3 perovskite structure oxides etc. [6–10]. Generally speaking, M^{n+}-doped $SrCeO_3$ has higher proton transfer numbers than those of M^{n+}-doped $BaCeO_3$ and can be used in gas sensors, gas separators, electrochemical membrane reactors and fuel cells [11]. Hung et al. found that $Sr(Ce_{0.6}Zr_{0.4})_{0.85}Y_{0.15}O_{3-\alpha}$ could be used in hydrogen separation membranes [12]. Matskevich et al. prepared $SrCe_{0.9}Lu_{0.1}O_{2.95}$ and found that Lu^{3+}-doping could increase the thermodynamic stability of $SrCeO_3$-based electrolyte [13]. The proton conductivities of M^{n+}-doped $SrZrO_3$ were lower than those of M^{n+}-doped $SrCeO_3$, however, their chemical stability and mechanical strength were better than those of $SrCeO_3$-based perovskite electrolytes [14]. Many studies have shown that double metal cation-doped $SrCeO_3$ has better electrical properties than single M^{n+}-doped $SrCeO_3$ [15–17]. Li et al. synthesized $SrCe_{0.9}Yb_{0.1}O_{3-\alpha}$ by a gel combustion method and the sintered temperature was lower than with the solid

state reaction method [18]. Therefore, $SrCe_{0.6}Zr_{0.3}Lu_{0.1}O_{3-\alpha}$ was synthesized by a citric-nitrate auto-combustion (CNA) method in this study.

$SrCeO_3$-based electrolytes have high ionic conductivities only when above 700 °C. Therefore, new composite electrolyte materials such as ceria-carbonates with high ionic conductivities at medium temperature (400–700 °C) have become the focus of solid oxide fuel cell research [19–25]. For example, Park et al. synthesized $Ce_{0.8}Nd_{0.2}O_{1.9}$-Li_2CO_3-Na_2CO_3 composite electrolyte which had good intermediate temperature electrical properties [23]. And we previously prepared M^{n+}(Gd^{3+}[26], Eu^{3+}[27])-doped $SrCeO_3$-NaCl-KCl composite electrolytes which had high ionic conductivities at intermediate temperatures (400–700 °C). Thus far, the study of lutetium and zirconium co-doped $SrCeO_3$-$(K/Li)_2CO_3$-(Na/K)Cl composite electrolyte has been insufficient.

In this study, a novel composite electrolyte $SrCe_{0.6}Zr_{0.3}Lu_{0.1}O_{3-\alpha}$-$(K/Li)_2CO_3$-(Na/K)Cl was prepared. The structure, morphology and medium temperature electrical properties of SCZLu-$(K/Li)_2CO_3$-(Na/K)Cl were investigated.

2. EXPERIMENTAL

According to the stoichiometric ratio of $SrCe_{0.6}Zr_{0.3}Lu_{0.1}O_{3-\alpha}$, Lu_2O_3 was liquefied in nitric acid and other metal ion nitrates were dissolved in water to form a uniform solution. Citric acid was added. And the solution was heated to evaporation and burnt to obtain the primary powder. Powder was pre-fired at 1200 °C for 5 h, then, sintered at 1540 °C for 5 h to obtain $SrCe_{0.6}Zr_{0.3}Lu_{0.1}O_{3-\alpha}$. Li_2CO_3-K_2CO_3 (1:1 mole ratio) and NaCl-KCl (1:1 mole ratio) were heated twice to form a uniform inorganic salt solid solution. The mixtures of $SrCe_{0.6}Zr_{0.3}Lu_{0.1}O_{3-\alpha}$, Li_2CO_3-K_2CO_3 and NaCl-KCl (weight ratio 7:1:2) were heated at 750 °C for 1 h to obtain SCZLu-$(K/Li)_2CO_3$-(Na/K)Cl pellets (thickness 1.2 mm, diameter 16mm).

The crystal structures of $SrCe_{0.6}Zr_{0.3}Lu_{0.1}O_{3-\alpha}$ and SCZLu-$(K/Li)_2CO_3$-(Na/K)Cl were determined by X-ray diffraction (XRD). A scanning electron microscope was used to characterize the morphologies of the sintered samples. In order to analyze the ionic conductivities, Pd-Ag paste was coated on both sides of the sintered samples and treated at 700 °C for 20 minutes. The AC impedance spectra of the samples were measured by a CHI660E electrochemical analyzer with Ag wires as the conductors. The test temperature range was 400–700 °C. The $\log \sigma \sim \log (pO_2)$ curves were obtained with different proportions of dry hydrogen, oxygen and nitrogen. Finally, hydrogen and oxygen were used as fuel and oxidant to test the fuel cell performance of SCZLu-$(K/Li)_2CO_3$-(Na/K)Cl.

3. RESULTS AND DISCUSSION

Fig. 1 shows the XRD diagrams of $SrCe_{0.6}Zr_{0.3}Lu_{0.1}O_{3-\alpha}$ and SCZLu-$(K/Li)_2CO_3$-(Na/K)Cl. The diffraction peaks of $SrCe_{0.6}Zr_{0.3}Lu_{0.1}O_{3-\alpha}$ are consistent with Xing et al. [15]. For SCZLu-$(K/Li)_2CO_3$-(Na/K)Cl, the extra peaks at 29°, 33° and 47° are obvious which come from crystalline KCl and NaCl respectively.

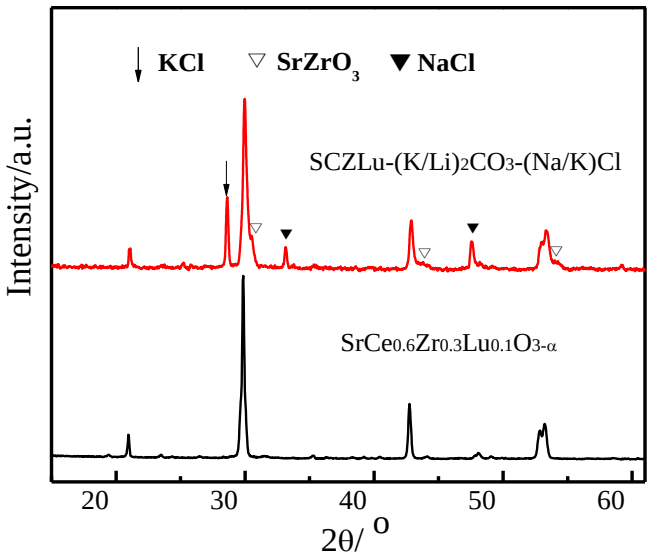

Figure 1. XRD patterns of $SrCe_{0.6}Zr_{0.3}Lu_{0.1}O_{3-\alpha}$ and SCZLu-$(K/Li)_2CO_3$-(Na/K)Cl.

There is no diffraction peak of carbonate in the XRD spectrum, so it can be inferred that carbonates exist between grain boundaries in amorphous form [22, 23, 28]. Huang et al. found that Li_2CO_3-Na_2CO_3 can decompose $BaCe_{0.7}Zr_{0.1}Y_{0.2}O_{3-\alpha}$ into $BaCO_3$ and CeO_2 [24]. Li_2CO_3-K_2CO_3 decreases the solid solution limitation between $SrZrO_3$ and $SrCeO_3$. Therefore, extra peaks of $SrZrO_3$ are also observed.

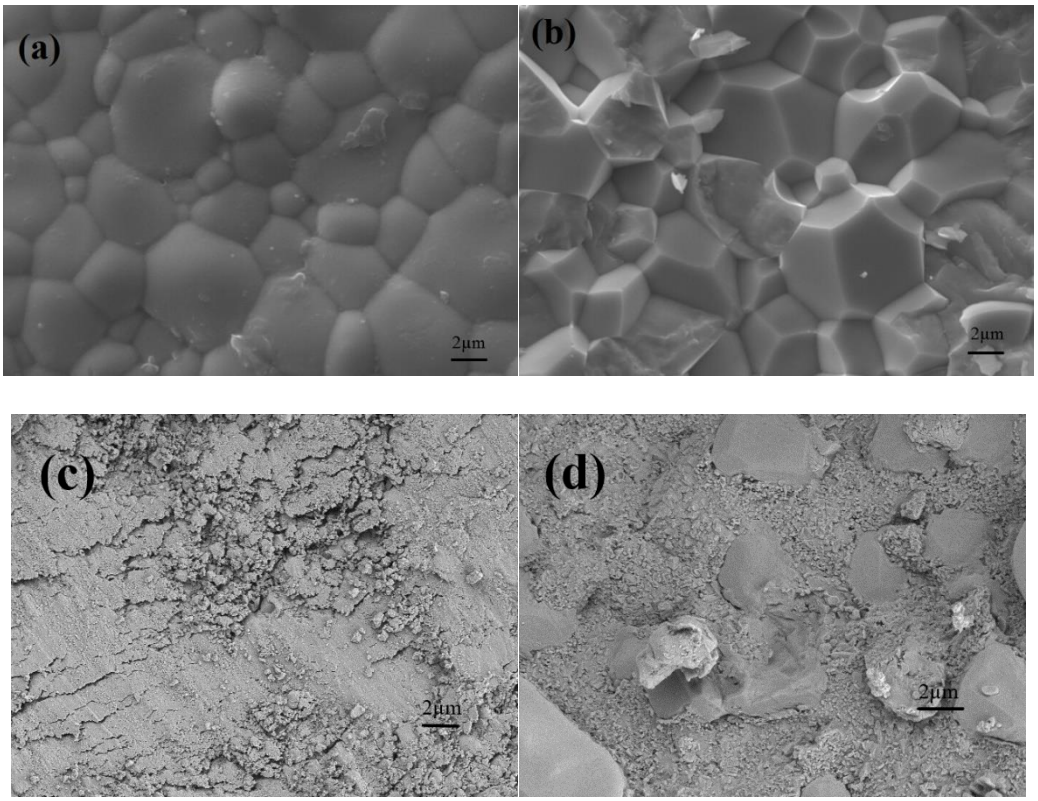

Figure 2. The external and cross-sectional SEM photos of $SrCe_{0.6}Zr_{0.3}Lu_{0.1}O_{3-\alpha}$ (a,b) and SCZLu-$(K/Li)_2CO_3$-(Na/K)Cl (c,d).

The external and cross-sectional SEM photos of $SrCe_{0.6}Zr_{0.3}Lu_{0.1}O_{3-\alpha}$ and SCZLu-$(K/Li)_2CO_3$-(Na/K)Cl are shown in Fig. 2. Fig. 2(a, b) are SEM diagrams of $SrCe_{0.6}Zr_{0.3}Lu_{0.1}O_{3-\alpha}$ prepared by CNA method after being sintered at 1540 °C for 5 h. Fig. 2(a, b) show that $SrCe_{0.6}Zr_{0.3}Lu_{0.1}O_{3-\alpha}$ has been densified and the grains of the sample are closely combined with regular shape and clear morphology. The distribution of grains is relatively uniform, and the grain size is concentrated between 1.5 μm and 4 μm. In the process of high temperature sintering, the molten carbonates and chlorides can flow among the $SrCe_{0.6}Zr_{0.3}Lu_{0.1}O_{3-\alpha}$ particles, fill the gaps and densify the composite electrolyte, as shown in Fig. 2(c, d) [21–25].

Fig. 3 shows the log (σT) ~ 1000 T^{-1} plots of $SrCe_{0.6}Zr_{0.3}Lu_{0.1}O_{3-\alpha}$, SCZLu-$(K/Li)_2CO_3$-(Na/K)Cl in air from 400 °C to 700 °C and the reported samples [26–27]. From Fig. 3, the conductivities of lutetium and zirconium co-doped $SrCeO_3$ are higher than $SrCe_{0.9}Gd_{0.1}O_{3-\alpha}$ prepared by a citric-nitrate auto-combustion process ($SrCe_{0.9}Gd_{0.1}O_{3-\alpha}$-CNA) and $SrCe_{0.9}Eu_{0.1}O_{3-\alpha}$ synthesized via a sol-gel method ($SrCe_{0.9}Eu_{0.1}O_{3-\alpha}$-SG) [26-27]. The result shows that $SrCeO_3$-based electrolyte materials with both electrical and chemical stability can be obtained by double doping. There is a turning point in the Arrhenius curve of SCZLu-$(K/Li)_2CO_3$-(Na/K)Cl at 500 °C. This is due to the melting of carbonate because the transition temperature is close to the melting point (490 °C) of $LiKCO_3$. The conductivities of SCZLu-$(K/Li)_2CO_3$-(Na/K)Cl are higher than those of pure $SrCeO_3$ in the temperature range of 500-700 °C. The conducting ions can be conducted through the interface and the bulk phase of SCZLu because inorganic salt is a solid solution above 500 °C [29]. The maximum conductivity of SCZLu-$(K/Li)_2CO_3$-(Na/K)Cl reached 2.5×10^{-2} S·cm^{-1} at 700 °C.

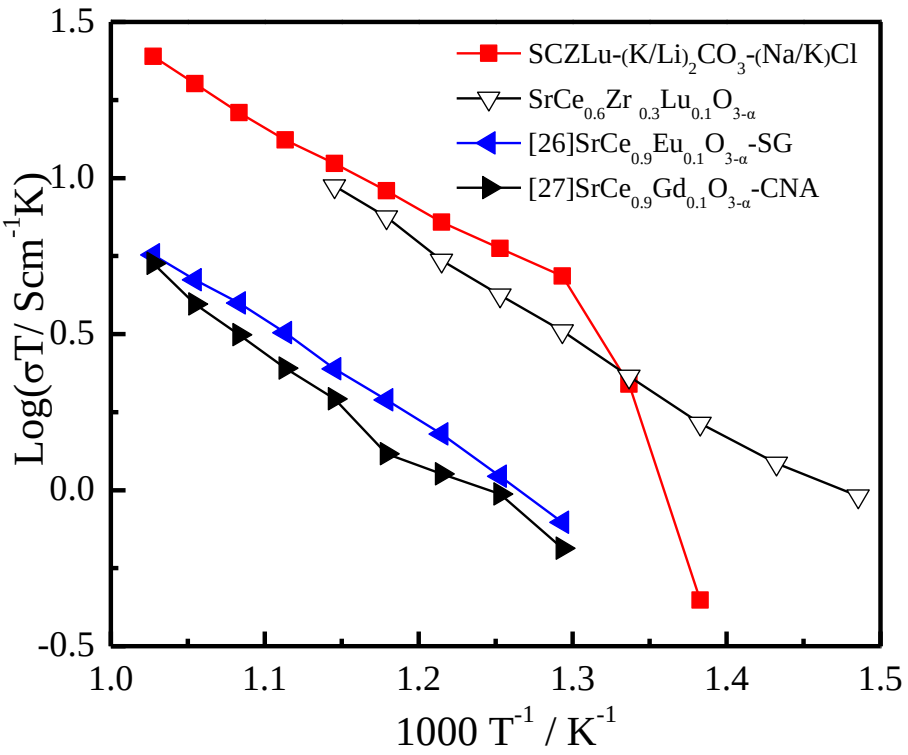

Figure 3. The log (σT) ~ 1000 T^{-1} plots of $SrCe_{0.6}Zr_{0.3}Lu_{0.1}O_{3-\alpha}$, SCZLu-$(K/Li)_2CO_3$-(Na/K)Cl in air from 400 °C to 700 °C and the reported samples.

Fig. 4 shows the log σ ~ log (pO_2) curves of $SrCe_{0.6}Zr_{0.3}Lu_{0.1}O_{3-\alpha}$ at 600 °C, SCZLu-$(K/Li)_2CO_3$-(Na/K)Cl at 700 °C and the reported $SrCe_{0.9}Eu_{0.1}O_{3-\alpha}$ at 700 °C. The log σ ~ log (pO_2) curve is usually studied to explore the ionic conduction in samples. Lin et al. studied 5mol % Tb^{3+}-doped $SrCeO_3$ and found that it is a pure protonic conductor with very low electronic conduction [30]. As shown in Fig. 4, the total conductivities in hydrogen, oxygen, air and nitrogen (pO_2 = 10^{-20} ~ 10^{0} atm) are almost the same, which shows that the electrolytes are pure ionic conductors.

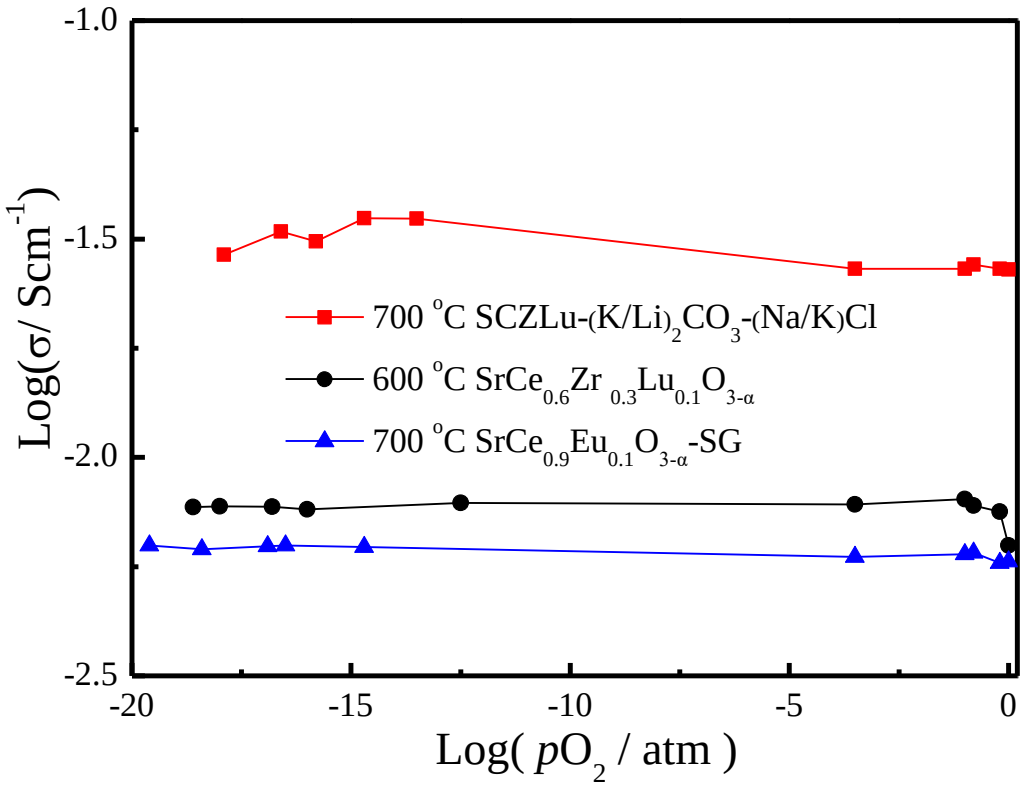

Figure 4. The log σ ~ log (pO_2) curves of $SrCe_{0.6}Zr_{0.3}Lu_{0.1}O_{3-\alpha}$ at 600 °C, SCZLu-$(K/Li)_2CO_3$-(Na/K)Cl at 700 °C and the reported $SrCe_{0.9}Eu_{0.1}O_{3-\alpha}$ at 700 °C.

Fig. 5 shows the *I-V-P* curves of SCZLu-$(K/Li)_2CO_3$-(Na/K)Cl and the reported $SrCe_{0.9}Eu_{0.1}O_{3-\alpha}$, $SrCe_{0.9}Gd_{0.1}O_{3-\alpha}$ at 700 °C. It can be seen from Fig. 5 that the *I-V* curve is basically straight, indicating that there is no electrode polarization and the microstructure of the electrode can meet the requirements. All the open circuit voltages are above 1.0 V, indicating that the electrolytes are basically airtight at 700 °C. The fuel cell using SCZLu-$(K/Li)_2CO_3$-(Na/K)Cl as electrolyte obtains the maximum power density of 50 mW·cm^{-2} at 700 °C. The $SrCe_{0.9}Gd_{0.1}O_{3-\alpha}$-CNA and $SrCe_{0.9}Eu_{0.1}O_{3-\alpha}$-SG only have 20 mW·$cm^{-2}$ and 13 mW·cm^{-2} under the same condition, respectively [26–27]. The power output of ours is higher than those of $SrCe_{0.9}Gd_{0.1}O_{3-\alpha}$ prepared by a citric-nitrate auto-combustion method ($SrCe_{0.6}Zr_{0.3}Lu_{0.1}O_{3-\alpha}$-CAN) [25], $SrCe_{0.9}Gd_{0.1}O_{3-\alpha}$-CNA [26] and $SrCe_{0.9}Eu_{0.1}O_{3-\alpha}$-SG [27] under the same condition (Table 1). It can be seen that the fuel cell performance of the composite electrolyte is better.

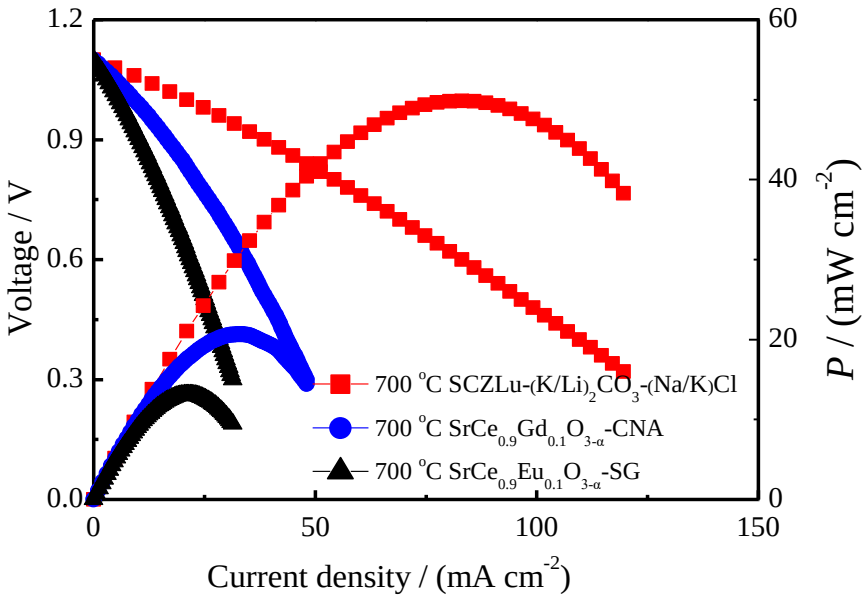

Figure 5. The *I-V-P* curves of SCZLu-$(K/Li)_2CO_3$-(Na/K)Cl and the reported $SrCe_{0.9}Eu_{0.1}O_{3-\alpha}$, $SrCe_{0.9}Gd_{0.1}O_{3-\alpha}$ at 700 °C.

Table 1 The highest power densities of SCZLu-$(K/Li)_2CO_3$-(Na/K)Cl and similar electrolytes in the literatures.

electrolytes	Highest power densities
SCZLu-$(K/Li)_2CO_3$-(Na/K)Cl	50 mW·cm^{-2}, 700 °C, in this work
$SrCe_{0.6}Zr_{0.3}Lu_{0.1}O_{3-\alpha}$-CNA	25 mW·cm^{-2}, 800 °C, [25]
$SrCe_{0.9}Gd_{0.1}O_{3-\alpha}$-CNA	20 mW·cm^{-2}, 700 °C, [26]
$SrCe_{0.9}Eu_{0.1}O_{3-\alpha}$-SG	13 mW·cm^{-2}, 700 °C, [27]

4. CONCLUSIONS

In this study, molten chlorides and carbonates was adopted to synthesize a new $SrCe_{0.6}Zr_{0.3}Lu_{0.1}O_{3-\alpha}$-$(K/Li)_2CO_3$-(Na/K)Cl composite electrolyte. The SEM photos showed that the molten carbonates and chlorides can flow among the $SrCe_{0.6}Zr_{0.3}Lu_{0.1}O_{3-\alpha}$ particles, fill the gaps and densify the composite electrolyte in the sintering process. The log σ ~ log (pO_2) results showed that SCZLu-$(K/Li)_2CO_3$-(Na/K)Cl is a pure ionic conductor. The maximum conductivity and power density of SCZLu-$(K/Li)_2CO_3$-(Na/K)Cl were 2.5×10^{-2} S·cm^{-1} and 50 mW·cm^{-2} at 700 °C, respectively.

ACKNOWLEDGEMENTS
This work was supported by the Natural Science Project of Anhui Province (No. KJ2018A0980, KJ2019A1273).

References

1. L. Bi, S.P. Shafi, E.H. Da'as and E. Traversa, *Small*, 14 (2018) 1801231.
2. C. Bernuy-Lopez, L. Rioja-Monllor, T. Nakamura, S. Ricote, R. O'Hayre, K. Amezawa, M. Einarsrud and T. Grande, *Materials*, 11 (2018) 196.
3. Y.P. Xia, Z.Z. Jin, H.Q. Wang, Z.Gong, H.L. Lv, R.R. Peng, W. Liu and L. Bi, *J. Mater. Chem. A*, 7 (2019) 16136.
4. Y. Tian, Z. Lü, X. Guo and P. Wu, *Int. J. Electrochem. Sci*., 14 (2019) 1093.
5. X. Xu, L. Bi and X.S. Zhao, *J. Membrane Sci.*, 558 (2018) 17.
6. A.A. Solovyev, S.V. Rabotkin, A.V. Shipilova and I.V. Ionov, *Int. J. Electrochem. Sci*., 14 (2019) 575.
7. X. Xu, H.Q. Wang, J.M. Ma, W.Y. Liu, X.F. Wang, M. Fronzi and L. Bi, *J. Mater. Chem. A*, 7 (2019) 18792.
8. H. Jiang and F. Zhang, *Int. J. Electrochem. Sci*., 15 (2020) 959.
9. J.M. Ma, Z.T. Tao, H.N. Kou, M. Fronzi and L. Bi, *Ceram. Int.*, 46 (2020) 4000.
10. H. Dai, H. Kou, Z. Tao, K. Liu, M. Xue, Q. Zhang, L. Bi, *Ceram. Int.*, doi: 10.1016/j.ceramint.2019.11.134.
11. K. Leonard, Y.-S. Lee, Y. Okuyama, K. Miyazaki and H. Matsumoto, *Int. J. Hydrogen. Energ*., 42 (2017) 3926.
12. I.-M. Hung, Y.-J. Chiang, J.S.-C. Jang, J.-C. Lin, S.-W. Lee, J.-K. Chang and C.-S. His, *J. Eur. Ceram. Soc.*, 35 (2015) 163.
13. N.I. Matskevich, T. Wolf, I.V. Vyazovkin and P. Adelmann, *J. Alloy Compd.*, 628 (2015) 126.
14. K.-T. Hsu, J.S.-C. Jang, Y.-J. Ren, P.-H. Tsai, C. Li, C.-J. Tseng, J.-C. Lin, C.-S. His and I-M. Hung, *J. Alloy Compd.*, 615 (2014) 5491.
15. W. Xing, P.I. Dahl, L.V. Roaas, M.-L. Fontaine, Y. Larring, P.P. Henriksen and R. Bredesen, *J. Membrane Sci.*, 473 (2015) 327.
16. Y. Okuyama, K. Isa, Y.S. Lee, T. Sakai and H. Matsumoto, *Solid State Ionics*, 275 (2015) 35.
17. P.S. Mahadik, D. Jain, A.N. Shirsat, N. Manoj, S. Varma, B.N. Wani and S.R. Bharadwaj, *Electrochimi. Acta*, 219 (2016) 614.
18. C. Zhang, S. Li, X.P. Liu, X.S. Zhao, D. He, H.C. Qiu, Q.H. Yu, S.M. Wang and L.J.Jiang, *Int. J. Hydrogen Energ.*, 38 (2013) 12921.
19. C. Slim, L. Baklouti, M. Cassir and A. Ringuedé, *Electrochim. Acta*, 123 (2014) 127.
20. F. Xie, C. Wang, Z. Mao and Z. Zhan, *Int. J. Hydrogen Energ.*, 39 (2014) 14397.
21. A.K. Ojha,V. Ponnilavan and S. Kannan, *Ceram. Int.*, 43 (2017) 686.
22. N.C.T. Martins, S. Rajesh and F.M.B. Marques, *Mater. Res. Bull.*, 70 (2015) 449.
23. J.T. Kim, T.H. Lee, K.Y. Park, Y. Seo, K.B. Kim, S.J. Song, B. Park and J.Y. Park, *J. Power Sources*, 275 (2015) 563.
24. Y. Hei, J. Huang, C. Wang and Z. Mao, *Int. J. Hydrogen Energ.*, 39 (2014) 14328.
25. D. Huang, Y. Han, F. Wu and H. Wang, *Ceram. Int.*, 45 (2019) 10149.
26. L. Sun, H.T. Wang, L.Q. Sheng and H.Q. Li, *Int. J. Electrochem. Sci.*, 12 (2017) 9689.
27. R. Shi, J. Liu, H. Wang, F. Wu, H. Miao and Y. Cui, *Int. J. Electrochem. Sci.*, 12 (2017) 11594.
28. S. Shawuti and M.A. Gulgun, *J. Power Sources.*, 267 (2014) 128.
29. X. Li, N. Xu, L. Zhang and K. Huang, *Electrochem. Commun.*, 13 (2011) 694.
30. X. Qi and Y.S. Lin, *Solid State Ionics*, 120 (1999) 85.